

# One-Step Synthesized Iron-Carbon Core-Shell Nanoparticles to Activate Persulfate for Effective Degradation of Tetrabromobisphenol A: Performance and Activation Mechanism

Yunjiang Yu <sup>1</sup>, Chang Liu <sup>1,2</sup>, Chenyu Yang <sup>1</sup>, Yang Yu <sup>3</sup>, Lun Lu <sup>1</sup>, Ruixue Ma <sup>1</sup>, and Liangzhong Li <sup>1,\*</sup>

<sup>1</sup> State Environmental Protection Key Laboratory of Environmental Pollution Health Risk Assessment, Center for Environmental Health Research, South China Institute of Environmental Sciences, Ministry of Ecology and Environment, Guangzhou 510655, China

<sup>2</sup> Inner Mongolia Autonomous Region Key Laboratory of Water Pollution Control, School of Ecology and Environment, Inner Mongolia University, Hohhot 010021, China

<sup>3</sup> Guangdong Key Laboratory of Environmental Pollution and Health, School of Environment Jinan University, Guangzhou 511443, China

\* Correspondence: liliangzhong@scies.org

**Table S1.** The summaries of reported organic pollutants degradation conditions and performances by iron-based activated PS degradation system.

**Table S2.** The basic information of the actual contaminated water.

**Figure S1** SEM and TEM image of Fe@MC.

**Figure S2** Hysteresis curves of Fe@MC nanocore-shell catalysts.

**Figure S3** TGA of Fe@MC .

**Figure S4** Full XPS spectrum Fe@MC.

**Figure S5** The relative content of C, O, Fe analyzed by SEM-EDX.

**Figure S6** N<sub>2</sub> sorption isotherms and pore size distributions of Fe@MC .

**Figure S7** Comparison of the effect of Fe@MC/PS system and Fe@MC on removing TBBPA.

**Figure S8** Recyclability and regeneration of Fe@MC core-shell nanoparticles on the degradation of TBBPA.

**Figure S9** The removal of TBBPA by Fe@MC/PS in actual contaminated water(a) and TOC removal efficiency with different PS concentration (b).

**Figure S10** Electron density Laplacian analysis (a) and projection map of electron localization function ELF (b) of TBBPA.

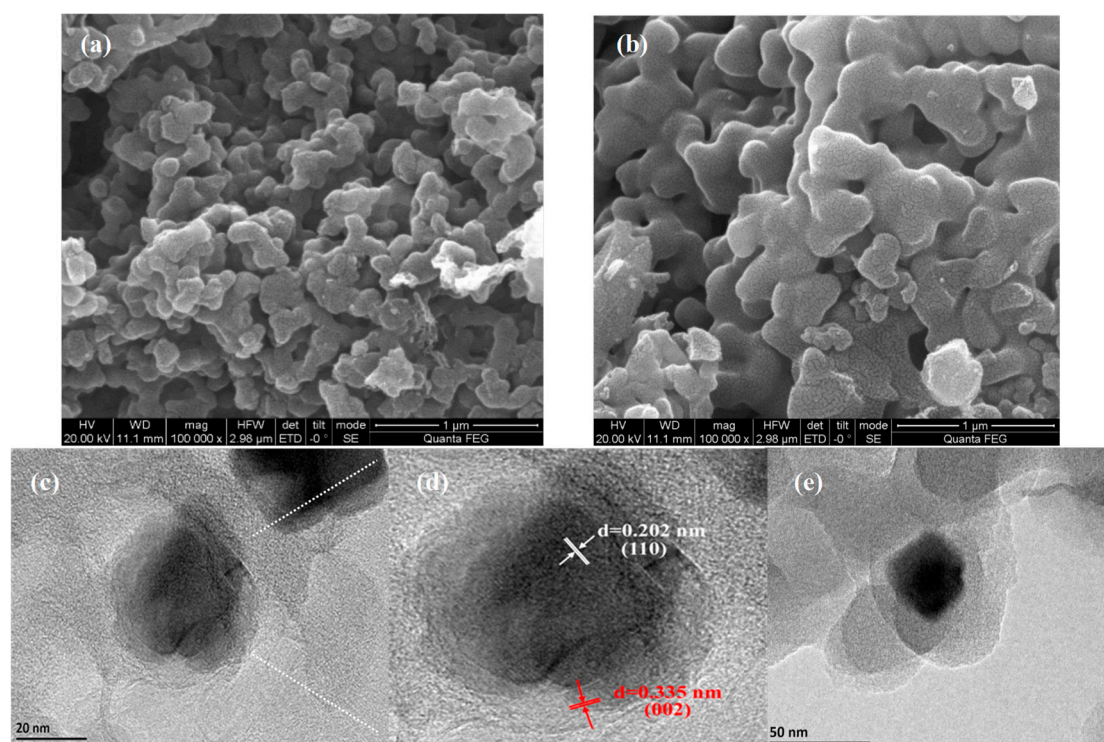
**Figure S11** Corresponding mass spectra and proposed structure of degradation products of TBBPA.

**Table S1.** The summaries of reported organic pollutants degradation conditions and performances by iron-based activators.

Catalyst	(g/L)	pollutant	(mg/L)	PS/PDS	pH	Reaction Time (min)	Removal efficiency (%)	Reference
Fe@MC	0.2	TBBPA	10	2.0	7.0	10	94.9	This work
MCFe	0.5	2,4,6-TCP	100	2.0	3	180	94.8	[1]
Fe@CN	0.1	BPA	20	0.5	6.8	60	96.0	[2]
Fe/Co@mHS	1	TBBPA	10	20.0	5	6	97.13	[3]
AC@Fe <sub>3</sub> O <sub>4</sub>	0.4	TC	10	40	3	180	99.8	[4]
FeO@Fe <sub>3</sub> O <sub>4</sub>	0.5	DPB	5	1.8	7	180	94.7	[5]

**Table S2.** The basic information of the actual contaminated water.

pH	Electrical conductivity (ms·cm <sup>-1</sup> )	COD (mg·L <sup>-1</sup> )	TOC (mg·L <sup>-1</sup> )	Turbidity (NTU)
8.22	1.10	202.0	160.1	87

**Figure S1.** SEM (a 800 °C, b 1200 °C) and TEM image of (b,c,d) Fe@MC.

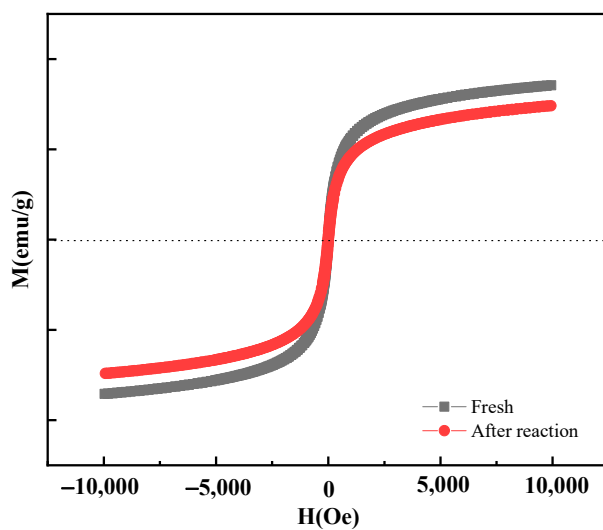


Figure S2. Hysteresis curve image of Fe@MC

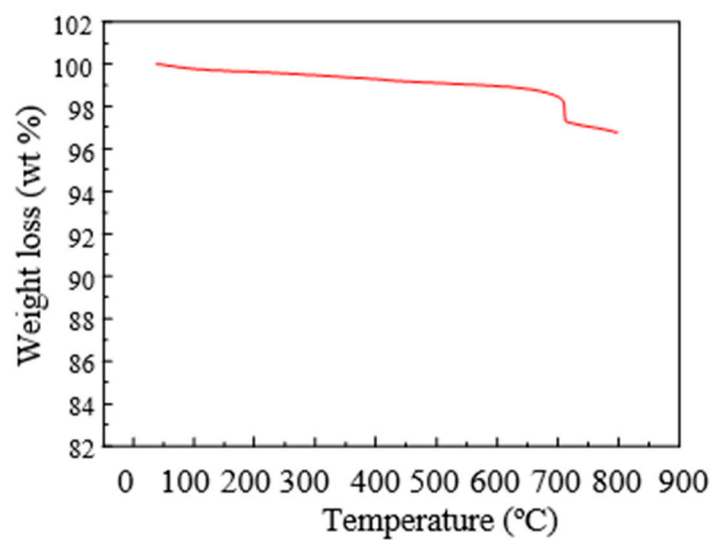
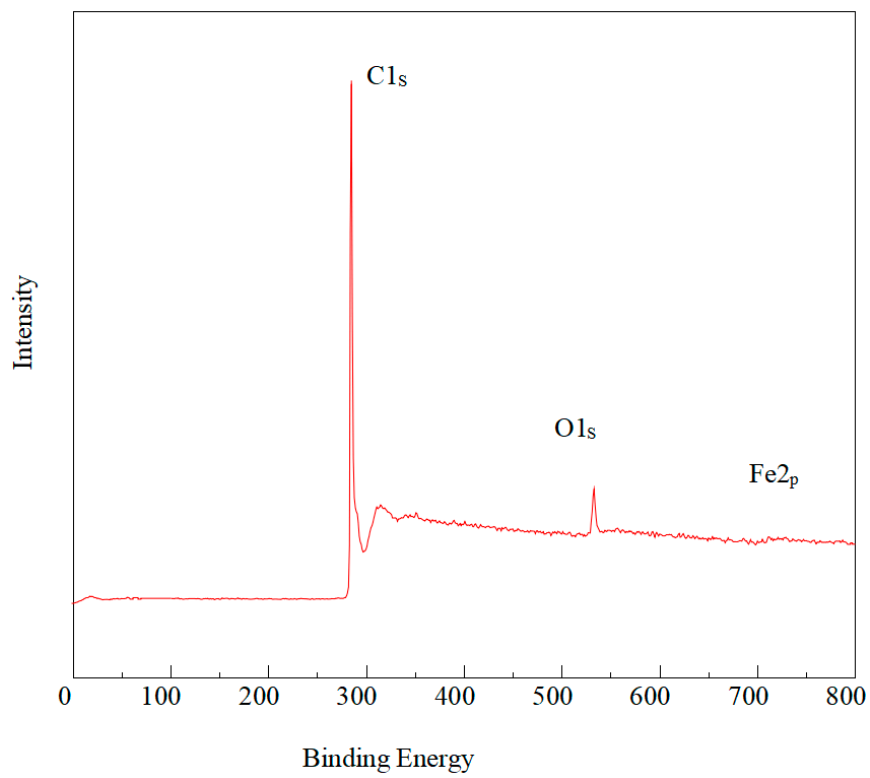
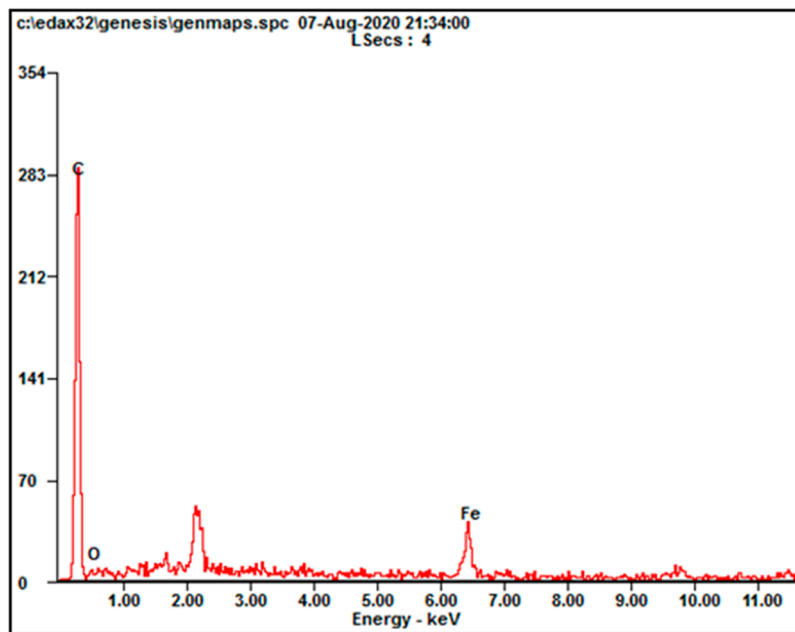


Figure S3. TGA of Fe@MC.



**Figure S4.** Full XPS spectrum Fe@MC .



	<i>Wt%</i>	<i>At%</i>
<b><i>CK</i></b>	88.49	95.77
<b><i>OK</i></b>	02.67	02.17
<b><i>FeK</i></b>	08.84	02.06
<b><i>Matrix</i></b>	Correction	ZAF

Figure S5. The relative content of C, O, Fe analyzed by SEM-EDX.

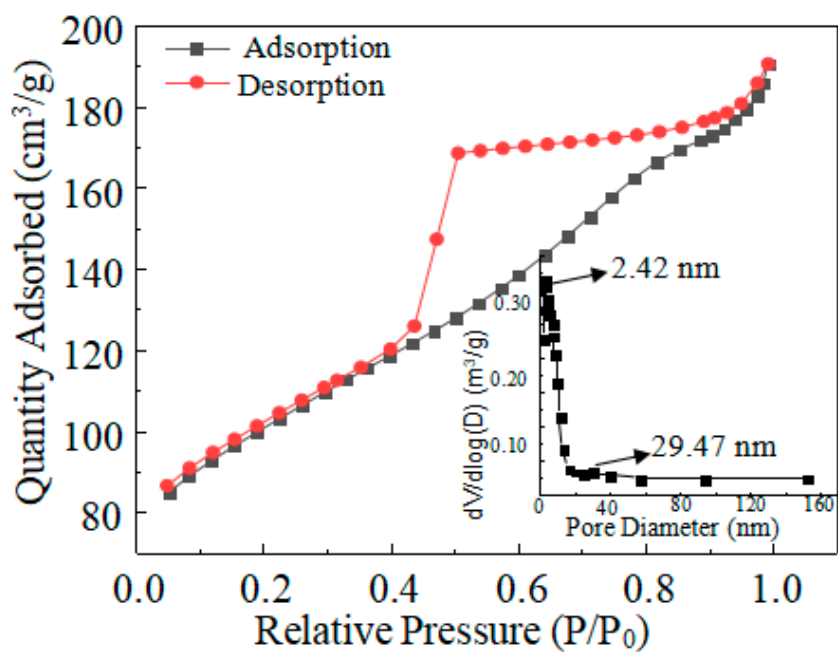


Figure S6. N<sub>2</sub> adsorption-desorption isotherms and pore size distributions of Fe@MC.

Figure S7.

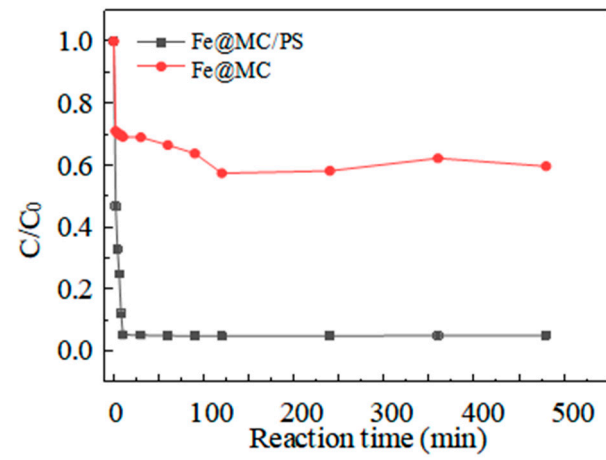


Figure S7. Effect of PS Addition on Removal of TBBPA

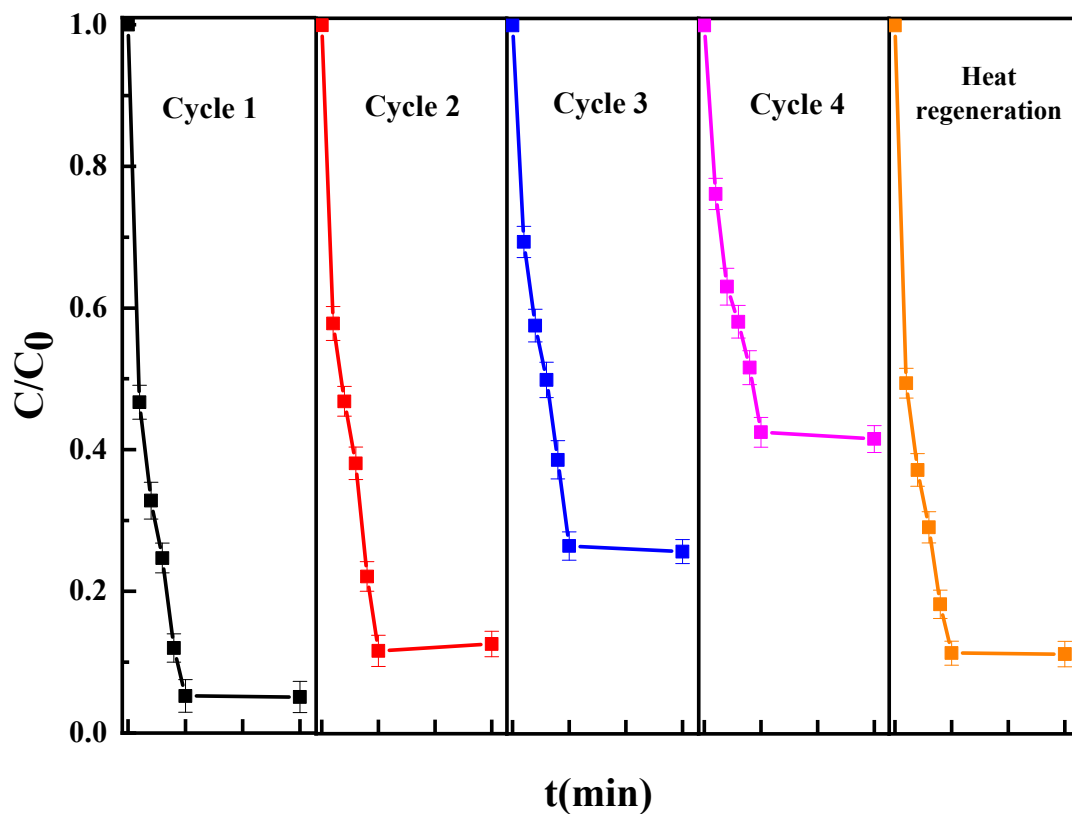


Figure S8. Recyclability and regeneration of Fe@MC

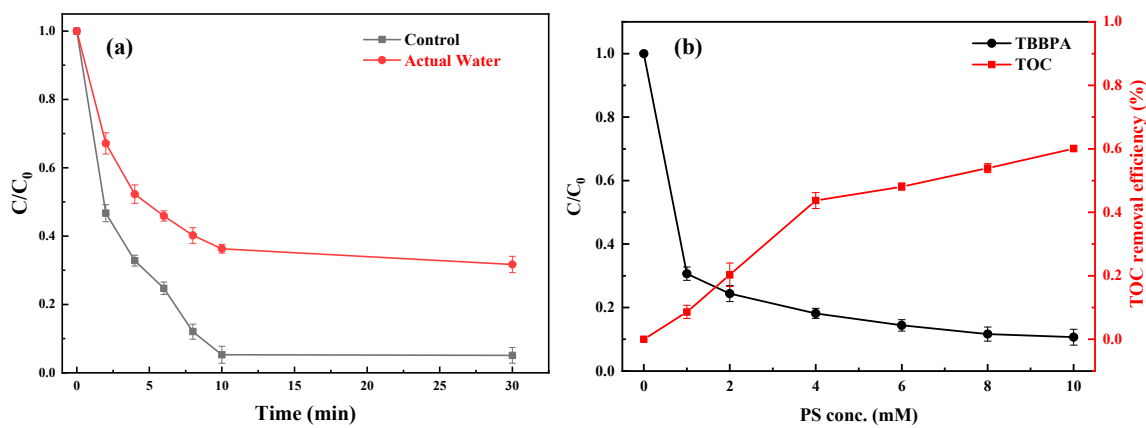
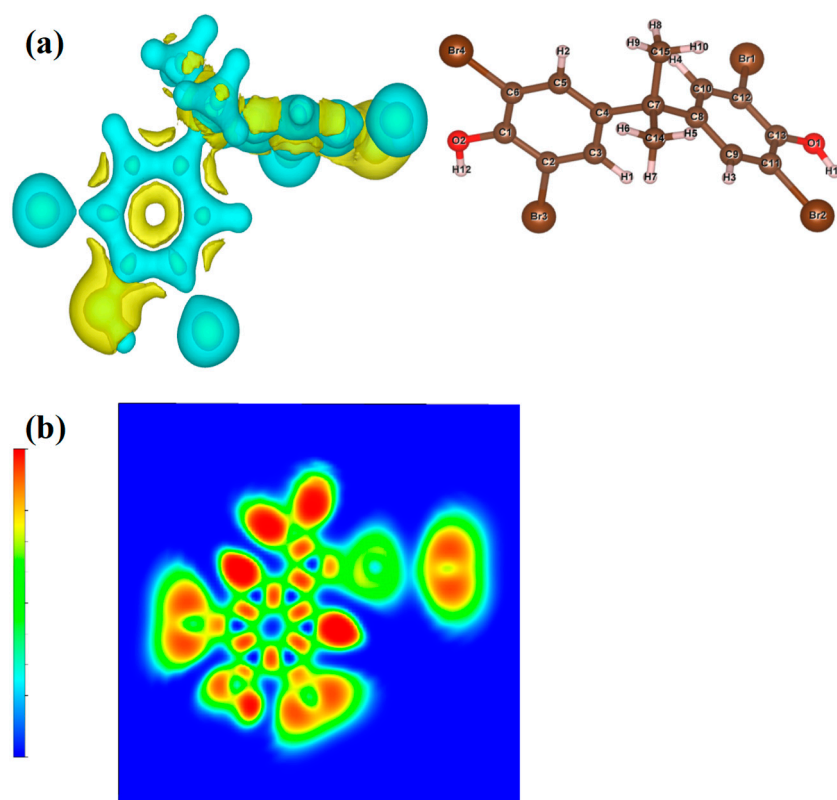
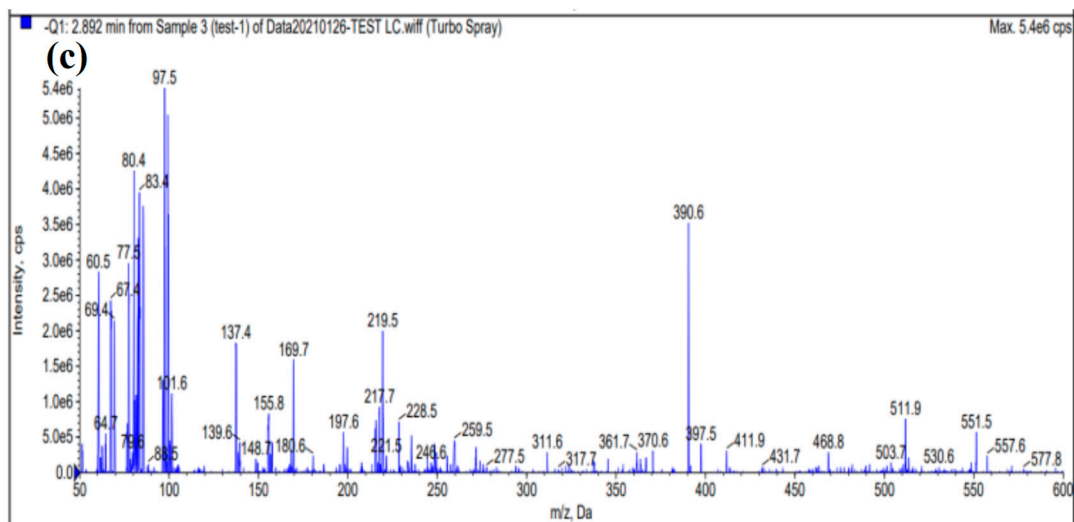
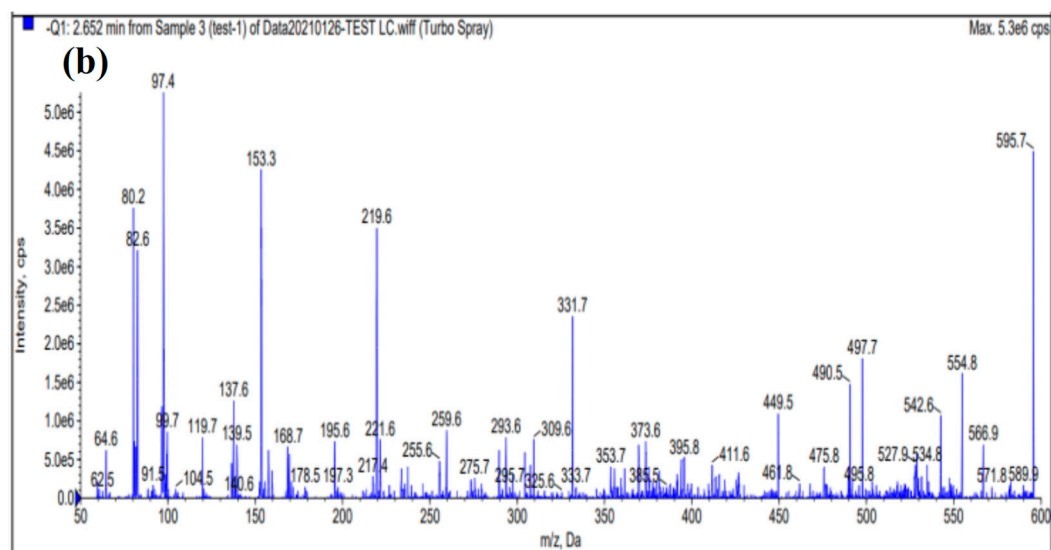
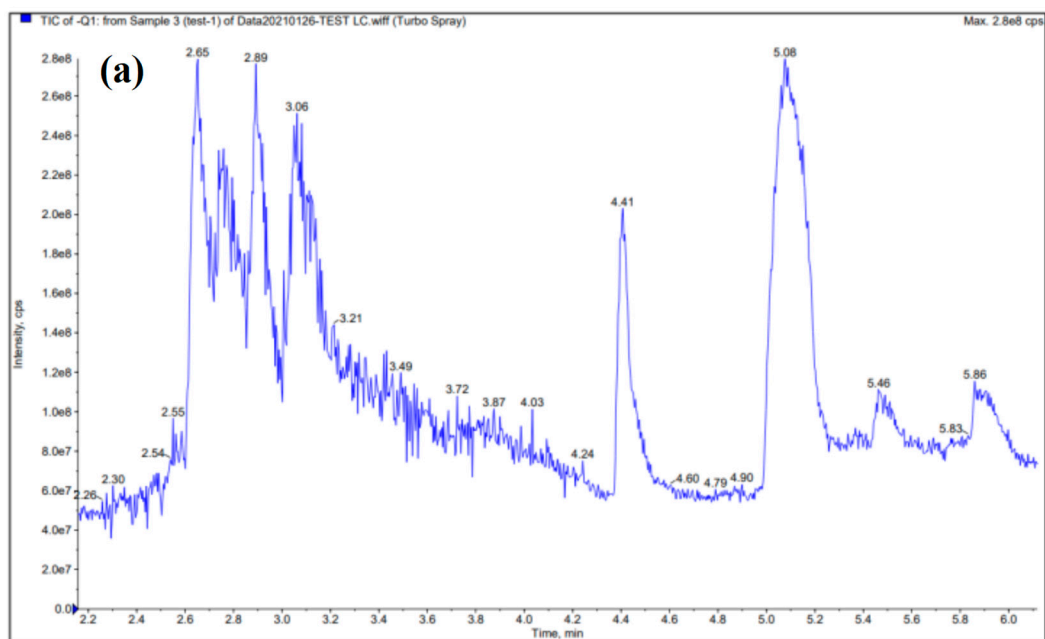
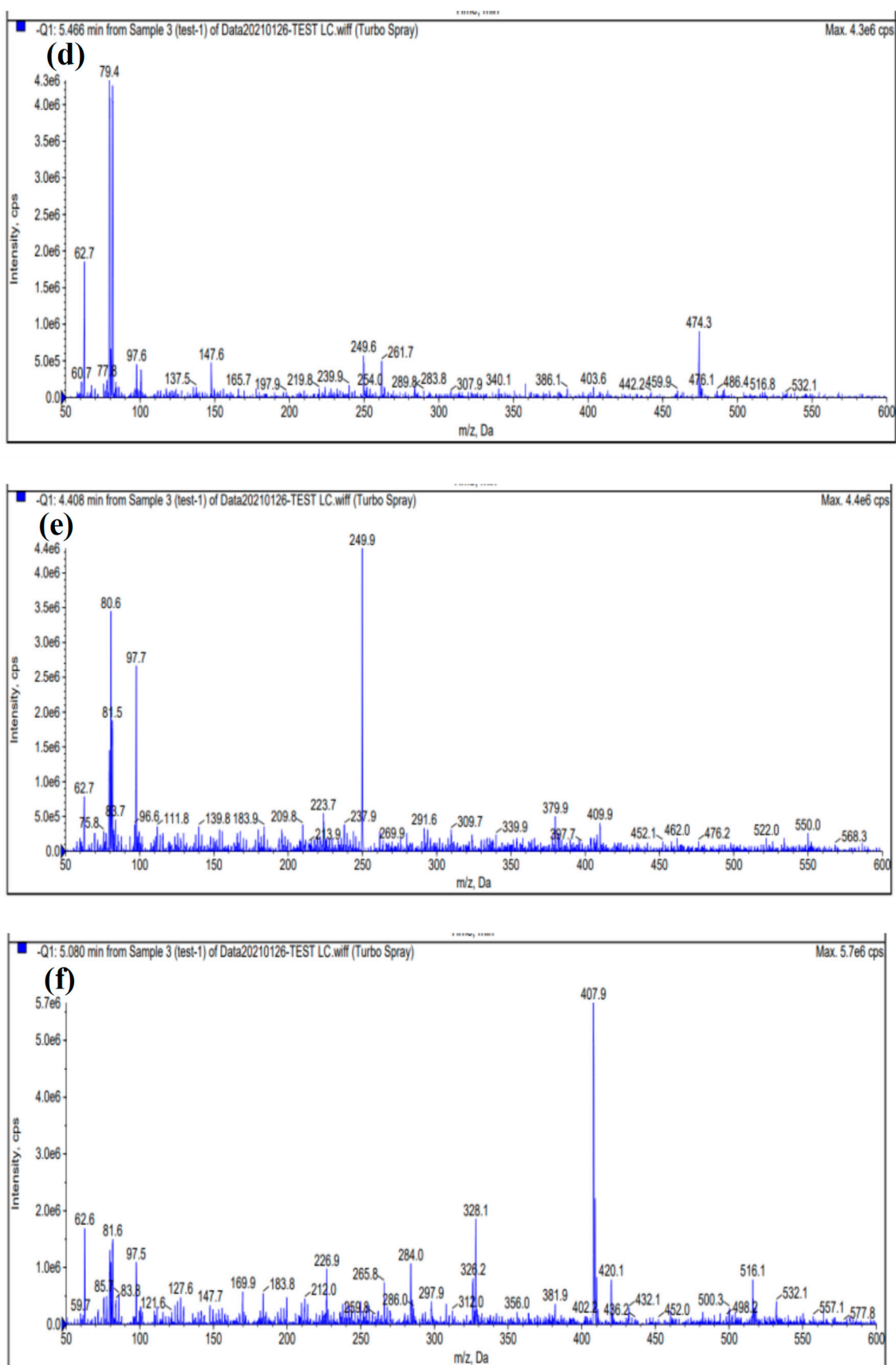


Figure S9. The removal of TBBPA by Fe@MC/PS in actual contaminated water(a) and TOC removal efficiency with different PS concentration (b).



**Figure S10.** Electron density Laplacian analysis (a) and projection map of electron localization function ELF (b) of TBBPA.





**Figure S11.** Corresponding mass spectra and structure of degradation products of TBBPA (The total mass spectra of degradation products (a) and each degradation product mass spectra (b,c,d,e,f)).

1. Wu, Y.W.; Chen, X.T.; Han, Y.; Yue, D.T.; Cao, X.D.; Zhao, Y.X.; Qian, X.F. Highly Efficient Utilization of Nano-Fe(0) Embedded in Mesoporous Carbon for Activation of Peroxydisulfate. *Environ. Sci. Technol.* **2019**, *53*, 9081–9090.
2. Liu, L.; Xu, X.; Li, Y.W.; Su, R.D.; Li, Q.; Zhou, W.Z.; Gao, B.Y.; Yue, Q. Y. One-step synthesis of “nuclear-shell” structure iron-carbon nanocomposite as a persulfate activator for bisphenol A degradation. *Chem. Eng. J.* **2020**, *382*, 122780.
3. Xiang, M.H.; Huang, M.F.; Li, H.; Wang, W.B.; Huang, Y.; Lu, Z.; Wang, C.; Si, R.F.; Cao, W. Nanoscale zero-valent iron/cobalt@mesoporous hydrated silica core-shell particles as a highly active heterogeneous Fenton catalyst for the degradation of tetrabromobisphenol A. *Chem. Eng. J.* **2021**, *417*, 129208.
4. Li, H.X.; Wan, J.Q.; Ma, Y.W.; Yan, W. Synthesis of novel core-shell Fe@Fe<sub>3</sub>O<sub>4</sub> as heterogeneous activator of persulfate for oxidation of dibutyl phthalate under neutral conditions. *Chem. Eng. J.* **2016**, *301*, 315–324.
5. Jonidi, J.A.; Kakavandi, B.; Jaafarzadeh, N.; Rezaei, K.R.; Ahmadi, M.; Akbar, B.A. Fenton-like catalytic oxidation of tetracycline by AC@Fe<sub>3</sub>O<sub>4</sub> as a heterogeneous persulfate activator: Adsorption and degradation studies. *Ind. Eng. Chem.* **2017**, *45*, 323–333.